Molecular BioSystems

Accepted Manuscript

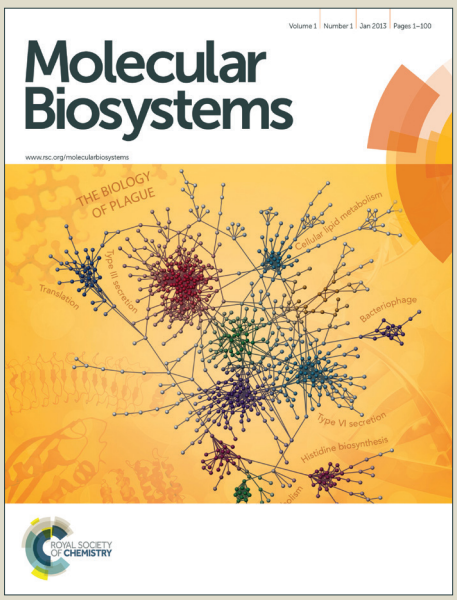

ROYAL SOCIETY OF CHEMISTRY

www.rsc.org/molecularbiosystems

NMR-based metabolomics approach to study the chronic toxicity of crude ricin from castor bean kernels on rats

Pingping Guo[a], Junsong Wang*[b], Ge Dong[a], Dandan Wei[a], Minghui Li[a], Minghua Yang[a], Lingyi Kong*[a]

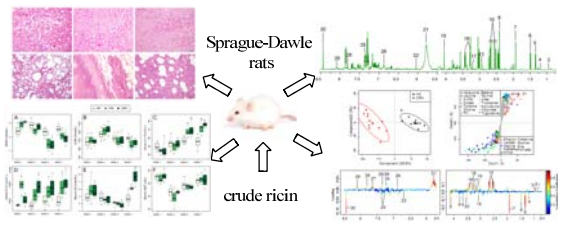

NMR based metabolomics approach combined with OSC-PLSDA was applied to investigate the chronic toxicity of crude ricin from castor bean kernels on rats for the first time.

NMR-based metabolomics approach to study the chronic toxicity of crude ricin from castor bean kernels on rats

Pingping Guo[a], Junsong Wang*[b], Ge Dong[a], Dandan Wei[a], Minghui Li[a], Minghua Yang[a], Lingyi Kong*[a]

Ricin, a large, water soluble toxic glycoprotein, is distributed majorly in the kernels of castor beans (the seeds of *Ricinus communis* L.), which has been used in traditional Chinese medicine (TCM) or other folk remedies throughout the world. The toxicity of crude ricin (CR) from castor bean kernels was investigated for the first time using a NMR-based metabolomic approach complemented with histopathological inspection and clinical chemistry. Chronic administration of CR could cause kidney and lung impairment, spleen and thymus dysfunction and diminished nutrient intake on rats. Orthogonal signal correction partial least-squares discriminant analysis (OSC-PLSDA) of metabolomic profiles of rat biofluids highlighted a number of metabolic disturbances induced by CR.

[a]*State Key Laboratory of Natural Medicines, Department of Natural Medicinal Chemistry, China Pharmaceutical University, 24 Tong Jia Xiang, Nanjing 210009, PR China. Fax: 86-25-8327-1405; Tel: 86-25-8327-1405; E-mail: cpu_lykong@126.com*

[b]*Center for Molecular Metabolism, School of Environmental & Biological Engineering, Nanjing University of Science & Technology, 200 Xiao Ling Wei Street, Nanjing 210094, PR China. E-mail: Fax: 86-25-8431-5512; Tel: 86-25-8431-5512; wang.junsong@gmail.com*

*Corresponding author: Prof. Junsong Wang and Prof. Lingyi Kong

Long-term CR treatment produced perturbations on energy metabolism, nitrogen metabolism, amino acid metabolism and kynurenine pathway, and evoked oxidative stress. These findings could explain well the CR induced nephrotoxicity and pulmonary toxicity, and provided several potential biomarkers for diagnostics of these toxicities. Such a ^{1}H NMR based metabolomics approach showed its ability to give a systematic and holistic view of the response of organism to drugs and suitable for dynamic studies on toxicological effect of TCM.

Introduction

Ricinus communisis L. (Euphorbiaceae) is a tropical perennial shrub that originated in Africa and cultivated in many tropical and subtropical regions around the world. The seeds of *R. communis*, also known as the castor beans, have been used in traditional Chinese medicine (TCM) or other folk remedies throughout the world as an emetic, a cathartic, a treatment for leprosy, and a cure for syphilis[1]. Castor beans are also toxic, and should be used with great care. The kernels of castor bean contain the highest concentration of ricin, a large, water soluble glycoprotein as a principal toxin of castor beans. Ricin poisoning has been described in humans and several other species of animals after ingestion of castor beans or residues from oil extraction[2-4]. Ricin is toxic by ingestion[5], inhalation[6], and injection[7, 8], and can be extracted and purified relatively easily from the castor bean kernels, which makes it of considerable interest for military or terrorist use[9]. Ricin presents two chains, A (RTA) and B (RTB), joined by a disulfide bond[10]. RTB is a lectin that binds specifically to galactoside present in glycoproteins on the cell surface, triggering

receptor-mediated endocytosis[11]; RTA is a 28S rRNA N-glycosidase that inhibits protein synthesis by depurination of a specific adenine residue, resulting in cell death[12-14]. The toxicity of ricin is ascribed majorly to its inhibition on protein synthesis, and also other mechanisms, such as apoptosis, direct cell membrane damage, alteration of membrane structure and function, and release of cytokine inflammatory mediators[15-18].

Besides traditional technologies for toxicological study, some newly arising "-omics" technologies, such as metabonomics, have been used[19, 20]. Metabonomics, by measuring the overall metabolic signature of biological samples[21], has demonstrated great potentials in many fields such as toxicological evaluation[22], disease process[23], and drug discovery[24, 25]. The application of metabonomics on the toxicological study has conspicuous superiority to traditional technologies due to its potential to dynamically monitor and globally evaluate the holistic metabolite changes after drug administration[26].

Most of the previous studies on ricin focused on its acute toxicity, its molecular structure and mechanism on cell model. However, the long-term toxicity of crude ricin (CR) from castor bean kernels, especially, on animal model has not been reported. ^{1}H NMR-based metabolomic approach combined with pattern recognition techniques was adopted in this study to investigate the chronic toxic effect of CR on rats.

Materials and methods

Chemicals and reagents

Castor beans were provided by Anguo Qirui Chinese Herbal Medicine Factory (Hebei, China) and identified by Professor Minjian Qin, Department of Medicinal Plants, China

Pharmaceutical University, Nanjing, China. The voucher specimen was deposited in Department of Natural Medicinal Chemistry, China Pharmaceutical University. The kits of blood urea nitrogen (BUN), urine urea nitrogen (UUN), lactic acid (LD), creatinine (Cr) and glutamyl transpeptidase (GGT) were purchased from Nanjing Jiancheng Bioengineering Institute (Nanjing, China). Deuterium oxide (D_2O, 99.9 %) was purchased from Sigma Chemical Co. (St. Louis, MO, USA). Ultra-pure distilled water, prepared from a Milli-Q purification system, was used.

Preparation of CR extract

CR was prepared in the laboratory as reported[27]. The dried and unshelled castor beans (40 g) were defatted twice with 400 ml petroleum ether. After stirring overnight at 4 ˚C, petroleum ether was eliminated by filtration and insoluble material was suspended in 800 ml phosphate buffer (2 mM, pH 7.0). After overnight stirring at 4 ˚C, the extract was centrifuged at 10,000 rpm at 4 ˚C for 30 min. The supernatant was stored at −20 ˚C before use. To ensure the activity of CR, the extraction was performed every week.

Animals and treatment

A total of 36 male Sprague-Dawley rats (200±20 g) were obtained from Comparative Medicine Centre of Yangzhou University (Yangzhou, China). All animals were reared in stainless steel wire-mesh cages in a well-ventilated room at a temperature of 25±3 ˚C and a relative humidity of 50±10%, with a 12 h light/12 h dark cycle. The studies were approved by the Animal Ethics Committee of China Pharmaceutical University, and were in

compliance with the National Institute of Health (NIH) guidelines for the Care and Use of Laboratory Animals.

The rats were acclimatized for 10 days with free access to food and water. After acclimatization, rats were randomly divided into three groups (twelve each) as follows: rats orally gavaged with CR at low dose of 0.25 g/kg/day (CRL), and high dose of 0.5 g/kg/day (CRH); and rats orally administered with approximately the same volume buffered saline as the normal control group (NC). For urine sample collection, rats were transferred to metabolism cages before collection, and transferred back to the stainless steel wire-mesh cages after collection. The oral gavage was performed consecutively for 8 weeks. The body weights were recorded daily.

Sample collection

On weeks 0, 1, 3, 5 and 7 after the administration of CR, the urine samples were collected for a 12 hours interval, during which the rats were deprived of food to avoid solid debris pollution, but were allowed to free access to tap water. After centrifugation (12,000 rpm, 10 min, 4 ˚C), the supernatant was stored at −80 ˚C.

Blood samples were taken from ocular vein of rats after 12 h fasting at week 0, 1, 3, 5 and 7 after the treatment. The serum samples were obtained by centrifugation (12,000 rpm, 10 min, 4 ˚C), stored at −80 ˚C before analysis.

Clinical chemistry

Blood and urine samples were collected in different time-points for clinical chemistry

evaluation. Serum and urine Cr, BUN and UUN for nephrotoxicity, serum GGT for hepatotoxicity and serum LD for abnormal energy metabolism were determined.

Histopathology

At the end of the study, the rats were fasted overnight and sacrificed after anesthetization by chloral hydrates (300 mg/kg, i.p.). The liver, lung, kidney, spleen and thymus were removed from the body at the time of death, flushed with ice-cold phosphate buffer solution, weighted, and then fixed in 10% neutral buffered formalin and embedded in paraffin. Serial sections of 5μm thickness were cut from tissue blocks and stained with hematoxylin eosin (HE).

Sample preparation and ^{1}H NMR spectroscopy

Urine samples were thawed at room temperature and 400 μl of each urine sample was mixed with 100 μl phosphate buffer solution (0.2 M Na_2HPO_4 and 0.2 M NaH_2PO_4, pH 7.0) and 100 μl TSP (3-trimethylsilyl-propionic acid, 0.05 % w/v in D_2O). D_2O was used for field frequency locking and phosphate buffer was added to minimize chemical shift variation due to differences in pH. The samples were vortexed and then centrifuged at 12,000 rpm for 10 min to remove any precipitates. The supernatant, c.a. 550 μl, was transferred into 5 mm NMR tubes. NMR spectra were recorded on a Bruker Av500 MHz spectrometer. For urine, the nuclear overhauser effect spectroscopy (NOESY) pulse sequence was applied to suppress the residual water signal. Free induction delays (FIDs) were collected with 128 transients into 32768 data points using a spectral width of 10000

Hz with a relaxation delay of 4 s, an acquisition time of 1.64 s, and a mixing time of 100 ms. All spectra were zero-filled to 32 k data points , and a line-broadening of 0.5 Hz was applied.

Serum samples were thawed and centrifuged at 12000 rpm for 10 min. The supernatant (350 µl) was transferred into 5 mm NMR tube containing 100 µl TSP (0.05%) and 150 µl D_2O. NMR spectra of these samples were also recorded on a Bruker AV 500 MHz spectrometer. A transverse relaxation-edited Call-Purcell-Meiboom-Gill (CPMG) sequence (90-(τ-80-τ)n-acquisition) with a total spin-echo delay (2nτ) of 10 ms was used to attenuate the broad signals from proteins, whereupon the signals of small molecule metabolites were clearly preserved. ^{1}H NMR spectra were measured with 128 scans into 32 K data points over a spectral width of 10000 Hz. The spectra were Fourier transformed after multiplying by an exponential window function with a line broadening of 0.5 Hz, and then were manually phased and baseline corrected using TOPSPIN software (version 3.0, Bruker Biospin, Germany).

Data processing and analysis

The ^{1}H NMR spectra were automatically reduced to ASCII files using MestReC (Beta version 3.7.4, Mestrelab Research SL), and were aligned based on least square minimization with shift corrected by the TSP signal. The region of residual water (4.2-5.7 ppm) signals was removed. The spectra were then binned (0.005 ppm bin width) and probability quotient normalized[28]. The mean-centered and Pareto-scaled NMR data were analyzed by supervised orthogonal signal correction partial least-squares discriminant

analysis (OSC-PLSDA). OSC-PLSDA, a supervised pattern recognition technique, was used to disclose the metabolic differences between classes, filtering out effects that are unrelated to interested response. The orthogonal signal correction (OSC) filters were developed to remove unwanted variation from spectral data[29]. OSC subtracts from X, factors that account for as much as possible of the variance in X and are orthogonal to Y. It is important to avoid over fitting after OSC treatment, to prevent poor predictive performance; hence, precise determination of the number of removed OSC factors is very important and here only one factor was removed. To assess the statistical significance of selected predictive quality parameters of the established OSC-PLSDA model, permutation testing and sevenfold cross-validation was carried out. The validity of the models against over fitting was assessed by the parameters R^2Y, and the predictive ability was described by Q^2Y. High Q^2Y values indicate that the differences between groups are significant. The overfitting cannot always be detected through cross-validation, but it can be detected using permutation tests[30-32]. Permutation testing is based on the comparison of the predictive capabilities of an OSC-PLSDA model using real class assignments to a number of models calculated after random permutation of the class labels. The performance measures are plotted on a histogram for visual assessment (Fig. 1). An empirical P value is often calculated by determining the number of times the permutated data yielded a better result than the one using the original labels. The observed statistic P values via permutation testing were all less than 0.05, thus confirming the validity of the OSC-PLSDA model. A parametric Student's t-test or a nonparametric Mann-Whitney test (dependent on the conformity to normal distribution) was performed on the signal integrals to evaluate the

difference of metabolites among groups. The OSC-PLSDA model parameters of comparison among different groups on week 7 were presented in Table 1, and the corresponding permutation testing statistics were shown in Fig. 1. Multivariate analysis was used to assess the integration area of metabolites over time and among groups using R software (http://cran.r-project.org/). Statistical differences between groups in clinical chemistry parameters, the body weights and the thymus and spleen indices were calculated by GraphPad Prism V 5.01 software (GraphPad Software Inc, San Diego, CA, USA), $p < 0.05$ was considered to be statistically significant. Values were expressed as mean±SD.

Results

Animal characteristics

During the experiment, alvi profluvium, emaciation bradykinesia and dyspnea were observed among the CR treated rats. The body weight (Fig. 2A) showed a significant decrease in rats administered with CR dose dependently. The thymus and spleen indices (Fig. 2B) of CR treated groups were significantly lower than the control group, indicating an immune toxicity induced by CR.

Clinical chemistry

The results of clinical chemistry were presented in Fig. 3. The level of BUN (Fig. 3A) on week 5 and 7, and UUN (Fig. 3B) on week 7 were decreased significantly ($p < 0.05$). Significantly increased level of serum Cr (Fig. 3C) on week 5 and 7, and increased level of urinary Cr (Fig. 3D) on week 7 were found in CRH and CRL group compared with NC.

The serum LD (Fig. 3E) showed significant increase in dosed groups on week 7. The level of LD in CRH was much higher than those in CRL, indicating a dose dependent toxicity of CR. Serum GGT (Fig. 3F) during the administration, however, did not show significant difference.

Histopathology

Histopathological changes in liver, spleen, lung, kidney and thymus were examined after HE staining. Kidney and lung showed severe pathological damage in dosed groups (Fig. 4); the other organs had no apparent change. CR caused severe tubular necrosis and epithelial cell edema (Fig. 4B and 4C) compared with NC (Fig. 4A). Severe alveolar wall thickening (Fig. 4F) and large amount of purulent exudates (Fig. 4E) was shown in the lung section of CR treated rats compared with NC rats (Fig. 4D). These facts combined with the clinical chemistry results demonstrated substantial kidney and lung damage after administration of CR.

Analysis of NMR spectra

Fig. 5 and Fig. 6 depict the normalized typical ^{1}H spectra of urine and serum samples obtained from healthy control and from CRL and CRH rats. Aided by statistical total correlation spectroscopy (STOSCY) technique[33], the assignments of metabolites were made by referencing reported data[34, 35] and searching publicly accessible metabolomic databases, such as HMDB (http://www.hmdb.ca), METLIN (http://metlin.scripps.edu) and KEGG (http://www.kegg.jp) and Chenomx NMR suit (Version 7.5, Chenomx, Inc.). The detailed

information of the metabolites was listed in Tables 2 and 3. Compared with the NC group, the increase of lactate, alanine, acetate and formate, and the decrease of citrate, urea and hippurate in urines of CRL and CRH group could be observed.

OSC-PLSDA score trajectory plot of all groups at all time points

The binned NMR data (mean-centered and pareto-scaled) were submitted to OSC-PLSDA. The dynamic metabolic events in rats were visualized by the OSC-PLSDA score trajectory plot (Fig. 7), where each spot represented the mean position of each group at each period, and the direction denoted by arrows represented the trend of the changing metabolite pattern. In the OSC-PLSDA score trajectory plots of urine and serum samples, the NC group was well separated from the CRL and CRH groups, which demonstrated that CR administration produced significant metabolic disturbances on rats. In the urine score trajectory plot (Fig. 7A), starting from week 0, the three groups moved apart, with the largest deviation in metabolomic profiles between the CR treated groups and the control group on week 1, then gradually reduced from week 1 to week 5, and increased again on week 7. This nonlinear shift of metabolic pattern showed complex response of the organism to counteract the toxicity. The OSC-PLSDA score trajectory plot of serum (Fig. 7B) showed a trend generally followed that of urine, but in a clear dose dependent manner.

^{1}H NMR metabolomics profiles of NC and CR treated groups on week 7

As shown in Figures 7A and 7B, notable toxicity induced by CR were achieved on week 7, therefore, the NMR data of week 7 were further analyzed by OSC-PLSDA. The

two-dimensional score plots of urine (Fig. 7C) and serum (Fig. 7D) data showed a clear separation of CR treated groups from NC, suggesting a severe metabolic perturbation induced by CR, and dose-dependently.

^{1}H NMR metabolomics profiles of CRH vs NC and CRL vs NC on week 7

The OSC-PLSDA analysis of urine samples showed an obvious separation between CRH and NC in the score plot (Fig. 8A). In order to identify the spectral bins that were responsible for the inter-class differences, the color encoded S-plot (Fig. 9), a scatter plot considering both the covariance (X axis) and correlation (Y axis) structure of loading profiles, was generated to filter the spectral bins of interested metabolites. The further away from the center, the more contribution of the metabolite to the clustering. In urine and serum samples, metabolites in the upper-right quadrant (positive correlation and covariance) are those significantly decreased in CRH (Fig. 9A and 9C) and CRL (Fig. 9B and 9D) vs NC, while those in the lower-left quadrant (negative correlation and covariance) were those increased in CR treated groups.

In the loading plots of CRH vs NC (Fig. 10A and 10B), metabolites in the positive region were deceased in CRH: isoleucine, leucine, 2-oxoglutarate (2-OG), citrate, choline, phosphocholine (PC), taurine, betaine, urea, tryptophan, kynurenine, tyrosine, hippurate, and trigonelline; whereas those in the negative region were increased in CRH: ethanol, lactate, alanine, acetate, creatinine, glycine, kynurenic acid (KYNA), phenylalanine (Phe) and formate.

The score plot of CRL vs NC (Fig. 8B) combined with the S-plot (Fig. 9B) and the

loading plots (Fig. 10C and 10D) disclosed metabolites in urine for the separation of CRL and NC: decreased levels of 2-OG, citrate, choline, phosphocholine (PC), taurine, betaine, urea, kynurenine, hippurate, and trigonelline in CRL; and elevated levels of lactate, alanine, acetate, dimethylglycine (DMG), creatinine, glycine, Phe and formate in CRL.

The OSC-PLSDA analysis was also performed on serum samples, to reveal detailed and statistically significant metabolite changes induced by CR. Fig. 8C illustrated an obvious group separation, suggesting a significant metabolic change due to CRH. Metabolites contributing to class separation could be easily discerned in the color coded loading plot (Fig. 10E) and S-plot (Fig. 9C). In the loading plot, metabolites in the negative region were elevated in CRH: leucine, isoleucine, valine, lactate, OAG (O-acetyl-glycoproteins), glutamate, glutamine, cysteine, creatine, creatinine, and glycine, and those in the positive region were reduced in CRH: LDL/VLDL (Low density lipoproteins/Very low density lipoproteins), NAG (N-Acetyl glycoproteins), 3HB (3-hydroxybutyrate), acetoacetate, pyruvate, betaine, GPC (glycerophosphorylcholine) and glucose.

The score plot of CRL vs NC (Fig. 9D), combined with S-plot (Fig.7D) and loading plot (Fig. 10F) discriminated metabolites for the separation in serum samples, and the tendency of the metabolites level changes were almost the same with CRH.

Discussion

The toxicity of CR was investigated firstly by histopathological inspection and clinical chemistry evaluation. Kidney histopathology showed severe tubular necrosis and epithelial cell edema in CR administered rats which was evidenced by decreased levels of BUN and

UUN, and increased level of Cr. Lung alveolar wall thickening was observed in CR treated rats, which together with the increased level of LD suggested a lung toxicity induced by CR. The decreased thymus and spleen indices demonstrated an immune toxicity of CR, which was also supported by the observed purulent exudates in lung. However, the spleen and thymus as well as the liver did not show significant histological alterations.

To investigate the variations of endogenous metabolites in CR treated rats, ^{1}H NMR-based metabolomics approach combined with multivariate statistical analysis was investigated to explore potential biomarkers and the affected metabolic pathways for the first time, and metabolic disturbance in energy metabolism, oxidative stress, nitrogen metabolism, amino acid metabolism and kynurenine pathway were induced by CR administration. Schematic diagram of the perturbed metabolic pathways was shown in Fig. 11.

Energy metabolism

In CR treated groups, significantly decreased levels of urinary citrate and 2-oxoglutarate (2-OG), and serum pyruvate and glucose, increased levels of urinary ethanol and, lactate and alanine in both serum and urine were observed. Taking part in the TCA cycle, the decrease of citrate and 2-OG suggested an inhibition of TCA cycle, the central metabolic energy pathway that promotes the oxidative decarboxylation of acetyl-CoA and produces reduced equivalents, NADH and $FADH_2$ to be used in respiratory chain[36]. Decreased urinary levels of TCA cycle intermediates have been observed in $HgCl_2$-induced nephrotoxicity and been attributed to toxin-induced alteration in tubular acid-base status or

the effects on the key enzymes in TCA cycle[37, 38]. Thus, the declined urine levels of citrate and 2-OG in this work might also be related with CR induced renal injury.

Glycolysis is the first step in glucose metabolism where one glucose molecule breakdown into two pyruvate. Pyruvate can be used to produce acetyl-CoA by pyruvate dehydrogenase complex, enters into TCA cycle, playing a key role in glucose aerobic oxidation and energy production. The inhibition of TCA cycle calls for the enhanced another source of energy supply by anoxic respiration where pyruvate could be converted to lactate via lactate dehydrogenase (LDH) or to alanine via alanine aminotransferase (ALT). The decrease of serum pyruvate and glucose, increase of lactate and alanine in serum and urine, and elevated ethanol in urine in CR treated rats demonstrated an enhanced anaerobic metabolism, which was also supported by the cage-side observations of dyspnea of rats and histopathology result of lung tissue.

However, anoxic respiration is a less efficient energy production way, which could not satisfy the energy demand of the body. Increased levels of creatinine and creatine in serum and urinary creatinine were observed in CR treated rats. Creatinine is a waste product formed by the slow spontaneous degradation of creatine-phosphate[39]. Creatine-phosphate functions as an energy conditioner that stores the energy of excess ATP[40, 41]. CR caused energy shortage, shifted the equilibrium of creatine-phosphate to produce ATP for energy demand and thus increased the total amount of free creatine which subsequently degraded to creatinine. As reported, urinary creatinine might be considered as a marker of renal function[42, 43], and renal impairment could cause a rise in serum creatinine and a concomitant rise in urine creatinine[44]. Additionally, increased excretion of urinary creatinine has also

been associated with oxidative stress[45-47].

We also observed decreased levels of lipids (LDL/VLDL), acetoacetate and 3-hydroxybutyrate (3HB) and increased level of acetate in CR treated rats. Acetoacetate and 3HB were ketones that were produced by lipids degradation through fatty acid oxidation. Ketones could be transferred from serum to muscle, kidney or brain where ketone body oxidation was happened to produce energy, thus serving as fuel in case of energy deficiency. As a result, the level of acetate, the end product of fatty acid oxidation, was increased in CR treated rats.

Significantly increased level of urinary formate, a byproduct in the production of acetate, was observed in dosed groups. Formate could be maintained at a normal level by oxidization via the folate pathway[48]. However, CR treatment caused interrupted nutrients absorption, thus induced folate deficiency that could not inhibit the increase of formate. Formate could disrupt mitochondrial electron transport and energy production by inhibiting cytochrome oxidase activity, the terminal electron acceptor of the electron transport chain. High level of formate could even cause cell death due to the final depletion of ATP.

Oxidative stress

It is reported that ricin could induce oxidative stress[17] and glutathione (GSH) depletion[49]. Depletion of GSH leads to increased level of ROS, which can induce cell death via lipid peroxidation and cellular protein alteration by initiating diverse stress-signaling pathways. We also observed in CR treated groups the increased serum levels of glutamine, glutamate, glycine and cysteine, which were the precursors of the major natural antioxidant GSH. The

increased levels of the precursors of GSH suggested an inhibition of GSH synthesis, leading to GSH deficiency.

A conspicuous decrease of choline and phosphocholine in urine of CR treated groups was observed. Synthesized in vivo or obtained by food intake, choline and phosphocholine are the components of phospholipids and are essential for the integrity of cell membranes. Oxidative damage of phospholipids of ROS is a severe menace to the viability of the cells, disrupting both the construction and function of membranes, eventually resulting in the rupture of cell and organelles, such as mitochondria[50]. Therefore, the decreased levels of choline and phosphocholine suggested a self healing mechanism of the body to repair the membranes damaged by ROS[51].

The urinary levels of betaine and taurine in CRH and CRL decreased dramatically in late stage of the dosing period. As a derivative of choline, betaine participates in the synthesis of methionine from homocysteine, and restores the level of S-adenosyl methionine (SAM), playing essential roles in phospholipid metabolism and membrane structure[52]. Taurine is one of the most abundant free amino acids presented in mammalian tissues with various biological functions, such as stabilizing cell membrane, scavenging oxygen free radicals[53], regulating intracellular osmostasis[54] and maintaining intracellular Ca^{2+} concentration[55]. Taurine and betaine have shown hepatoprotective effects against oxidative stress such as lipid peroxidation[56] and prooxidant status[52], and hence, their decreased levels suggested their over-consumption to counteract the damage due to oxidative stress in CR treated rats.

Nitrogen metabolism

Significantly decreased level of urinary urea was observed, together with decreased levels of BUN and UUN in clinical chemistry. CR is commonly used for the treatment of astriction, and its overuse may induce intestine and stomach dysfunction, such as alvi profluvium, emaciation and bradykinesia, which was observed in this study. The levels of BUN and UUN were significantly decreased in CR treated rats. It is reported that adequate protein intake may induce the increase level of BUN and limited energy intake would upset this relationship[57]. These facts together with severely decreased body weight of CR treated rats demonstrated that the absorption of nutrients was greatly affected by overdose of CR, which was also supported by the greatly decreased level of urinary urea, the principal end product of protein catabolism.

Amino acid metabolism

Levels of serum BCAAs (leucine, isoleucine and valine) were increased in dosed groups. BCAAs are essential amino acids that are important for protein synthesis. Their increase suggested an inhibition of protein synthesis, consistent with the report that ricin could irreversibly inhibits protein synthesis causing cell death[14, 58, 59]. As the most important precursors for gluconeogenesis, the increase of BCAAs and decrease of glucose might also indicate an inhibited gluconeogenesis.

The urinary level of alanine in CR treated rats was increased as compared with the normal control rats. Alanine is a nonessential amino acid that is made in the body by conversion of pyruvate. It is highly concentrated in muscle and is one of the most important

amino acids released by muscle, functioning as a major energy source. Holmes et al. suggested that elevation in urinary alanine should be used as a biomarker of renal cortical toxicity, especially during a late stage after dosing[60]. The elevation of urinary alanine level has also been observed in nephrotoxicity caused by two common nephrotoxicity drugs, $HgCl_2$ and gentamicin[61, 62]. We also observed obvious endothelial cell edema and necrosis in kidney tubules of CR treated rats. Amino acids are normally reabsorbed by active transport of renal tubule. The increased alanine level thus demonstrated kidney impairment produced by CR.

Increased level of phenylalanine and decreased level of tyrosine in urine of CR treated rats were observed. Tyrosine is referred to as a semiessential or conditionally indispensable amino acid because it can only be synthesized by the hydroxylation of phenylalanine catalyzed by phenylalanine hydroxylase (PAH). As contrast, phenylalanine is an essential amino acid, and has to be obtained by food intake. Considering the affected nutrition absorption by CR, the increase of phenylalanine and decrease of tyrosine suggested an inhibition of PAH, which was observed in chronic kidney failure[63], and thus demonstrated a chronic renal damage induced by long-term CR treatment.

Kynurenine pathway

The decreased urinary levels of tryptophan and kynurenine, and increased level of kynurenic acid were observed in CR treated rats. Kynurenine is an intermediate of a tryptophan metabolism branch which is called kynurenine pathway. Indoleamine-2, 3-dioxygenase (IDO) is the first enzyme in kynurenine pathway, which converts tryptophan

to kynurenine. It has been reported that renal damage is associated with increased proinflammatory cytokines, which activate IDO[64]. The decrease in tryptophan level suggested an activated IDO to enhance the conversion from tryptophan to kynurenine. The actually decreased level of kynurenine in CR treated groups indicated a facilitated further conversion of kynurenine, producing kynurenic acid and 3-hydroxykynurenine[65]. Noteworthily, 3-hydroxykynurenine was reported to produce oxidative stress and led to renal cell death, which were frequently associated with renal damage[66, 67]. These kynurenine metabolites may have the potential to be biomarkers for clinical diagnosis of renal damage diseases and efficacy assess of their treatment.

In summary, long-term treatment with CR could cause kidney and lung impairment, spleen and thymus dysfunction and diminished nutrient intake. Interrupted oxygen ingest shifted the energy metabolism from aerobic to anaerobic state. CR treatment induced excessive ROS release causing membranes damage and GSH depletion, finally provoked cell and organelles rupture. Diminished nutrient intake of rats led to nitrogen metabolism depletion. Amino acid metabolism was perturbed, resulting from inhibited protein synthesis and renal injury. Disordered kynurenine pathway was found to be closely related with renal damage induced by CR treatment.

Conclusion

In conjunction with histopathological inspection and clinical chemistry assays, ^{1}H NMR based metabonomic approach was applied for the first time to study the toxicity of CR.

Statistical analyses of metabolomic profiles of rat biofluids highlighted a number of metabolic disturbances induced by CR. Long-term CR administration produced perturbations on energy metabolism, oxidative stress, nitrogen metabolism, amino acid metabolism and kynurenine pathway. These findings could explain well the CR induced nephrotoxicity and pulmonary toxicity, and provided several potential biomarkers for diagnostics of these toxicities. Such a ^{1}H NMR based metabolomics approach showed its ability to give a systematic and holistic view of the biochemical effect of drugs on organism and suitable for the investigation of the toxicological effect of drugs especially TCM.

Acknowledgements

The present study was funded by National Science Foundation of China (NSFC) grant 81173526, the Program for New Century Excellent Talents in University (NCET-11-0738), the Fundamental Research Funds for the Central Universities (No. 30920130112014), the Priority Academic Program Development of Jiangsu Higher Education Institutions (PAPD), and the Program for Changjiang Scholars and Innovative Research Team in University (PCSIRT-IRT1193).

References

1. A. Scarpa and A. Guerci, *J Ethnopharmacol*, 1982, **5**, 117-137.
2. B. Soto-Blanco, I. L. Sinhorini, S. L. Gorniak and B. Schumaher-Henrique, *Vet Hum Toxicol*, 2002, **44**, 155-156.
3. T. Garland and E. Bailey, *Rev Sci Tech Oie*, 2006, **25**, 341-351.
4. S. Roels, V. Coopman, P. Vanhaelen and J. Cordonnier, *J Vet Diagn Invest*, 2010, **22**, 466-468.
5. S. M. Bradberry, K. J. Dickers, P. Rice, G. D. Griffiths and J. A. Vale, *Toxicol Rev*, 2003, **22**, 65-70.
6. J. M. Benson, A. P. Gomez, M. L. Wolf, B. M. Tibbetts and T. H. March, *Inhal Toxicol*, 2011, **23**, 247-256.
7. J. Zhan and P. Zhou, *Toxicology*, 2003, **186**, 119-123.
8. M. Alipour, K. Pucaj, M. G. Smith and Z. E. Suntres, *Drug Chem Toxicol*, 2013, **36**, 224-230.

9. J. Audi, M. Belson, M. Patel, J. Schier and J. Osterloh, *Jama*, 2005, **294**, 2342-2351.
10. S. Olsnes, *Toxicon*, 2004, **44**, 361-370.
11. M. Ishiguro, M. Tomi, G. Funatsu and M. Funatsu, *Toxicon*, 1976, **14**, 157-165.
12. Y. Endo and K. Tsurugi, *J Biol Chem*, 1987, **262**, 8128-8130.
13. J. M. Lord, L. M. Roberts and J. D. Robertus, *Faseb J*, 1994, **8**, 201-208.
14. Y. Endo, R. Morishita, K. M. Imashevich and S. Yoshinari, *J Toxicol-toxin Rev*, 1998, **17**, 427-439.
15. H. Morino, R. Sakakibara and M. Ishiguro, *Biol Pharm Bull*, 1995, **18**, 1770-1770.
16. J. N. Hughes, C. D. Lindsay and G. D. Griffiths, *Hum Exp Toxicol*, 1996, **15**, 443-451.
17. O. Kumar, K. Sugendran and R. Vijayaraghavan, *Toxicon*, 2003, **41**, 333-338.
18. S. Lombard, M. Helmy and G. Pieroni, *Biochem. J*, 2001, **358**, 773-781.
19. L. Suter, L. E. Babiss and E. B. Wheeldon, *Chem Biol*, 2004, **11**, 161-171.
20. S. Ekins, Y. Nikolsky and T. Nikolskaya, *Trends Pharmacol Sci*, 2005, **26**, 202-209.
21. A. Sreekumar, L. M. Poisson, T. M. Rajendiran, A. P. Khan, Q. Cao, J. Yu, B. Laxman, R. Mehra, R. J. Lonigro and Y. Li, *Nature*, 2009, **457**, 910-914.
22. J. P. Shockcor and E. Holmes, *Curr Top Med Chem*, 2002, **2**, 35-51.
23. A. K. Arakaki, J. Skolnick and J. F. McDonald, *Nature*, 2008, **456**, 443-443.
24. D. J. Oliver, B. Nikolau and E. S. Wurtele, *Metab Eng*, 2002, **4**, 98-106.
25. J. C. Lindon, J. K. Nicholson, E. Holmes, H. Antti, M. E. Bollard, H. Keun, O. Beckonert, T. M. Ebbels, M. D. Reilly, D. Robertson, G. J. Stevens, P. Luke, A. P. Breau, G. H. Cantor, R. H. Bible, U. Niederhauser, H. Senn, G. Schlotterbeck, U. G. Sidelmann, S. M. Laursen, A. Tymiak, B. D. Car, L. Lehman-McKeeman, J. M. Colet, A. Loukaci and C. Thomas, *Toxicol Appl Pharm*, 2003, **187**, 137-146.
26. L. Li, B. Sun, Q. Zhang, J. Fang, K. Ma, Y. Li, H. Chen, F. Dong, Y. Gao, F. Li and X. Yan, *J Ethnopharmacol*, 2008, **116**, 561-568.
27. A. S. Salhab, S. O. Al-Tamimi, M. N. Gharaibehand Maha and S. Shomaf, *Contraception*, 1998, **58**, 193-197.
28. F. Dieterle, A. Ross, G. Schlotterbeck and H. Senn, *Anal Chem*, 2006, **78**, 4281-4290.
29. T. Fearn, *Chemometr Intell Lab*, 2000, **50**, 47-52.
30. J. A. Westerhuis, H. C. Hoefsloot, S. Smit, D. J. Vis, A. K. Smilde, E. J. van Velzen, J. P. van Duijnhoven and F. A. van Dorsten, *Metabolomics*, 2008, **4**, 81-89.
31. S. Bijlsma, I. Bobeldijk, E. R. Verheij, R. Ramaker, S. Kochhar, I. A. Macdonald, B. van Ommen and A. K. Smilde, *Anal Chem*, 2006, **78**, 567-574.
32. J. Xia, N. Psychogios, N. Young and D. S. Wishart, *Nucleic Acids Res*, 2009, **37**, W652-W660.
33. O. Cloarec, M.-E. Dumas, A. Craig, R. H. Barton, J. Trygg, J. Hudson, C. Blancher, D. Gauguier, J. C. Lindon and E. Holmes, *Anal Chem*, 2005, **77**, 1282-1289.
34. E. Holmes, P. J. D. Foxall, M. Spraul, R. D. Farrant, J. K. Nicholson and J. C. Lindon, *J Pharmaceut Biomed*, 1997, **15**, 1647-1659.
35. J. K. Nicholson, P. J. Foxall, M. Spraul, R. D. Farrant and J. C. Lindon, *Anal Chem*, 1995, **67**, 793-811.
36. H. Krebs, *Adv Enzyme Regul*, 1970, **8**, 335-353.
37. J. K. Nicholson, J. A. Timbrell and P. J. Sadler, *Mol Pharmacol*, 1985, **27**, 644-651.
38. E. Holmes, F. Bonner, K. Gartland and J. Nicholson, *J Pharmaceut Biomed*, 1990, **8**, 959-962.
39. M. Wyss and R. Kaddurah-Daouk, *Physiol Rev*, 2000, **80**, 1107-1213.
40. C. Ma, K. Bi, M. Zhang, D. Su, X. Fan, W. Ji, C. Wang and X. Chen, *J Ethnopharmacol*, 2010, **130**, 134-142.
41. C. Ma, K. Bi, M. Zhang, D. Su, X. Fan, W. Ji, C. Wang and X. Chen, *J Pharmaceut Biomed*, 2010, **53**, 559-566.
42. J. Bell, P. Sadler, V. Morris and O. Levander, *Magnet Reson Med*, 1991, **17**, 414-422.
43. Y. Zhang, S. Yan, X. Gao, X. Xiong, W. Dai, X. Liu, L. Li, W. Zhang and C. Mei, *Aging Clin Exp Res*, 2012, **24**, 79-84.

44. M. I. Shariff, A. I. Gomaa, I. J. Cox, M. Patel, H. R. Williams, M. M. Crossey, A. V. Thillainayagam, H. C. Thomas, I. Waked and S. A. Khan, *J Proteome Res*, 2011, **10**, 1828-1836.
45. L. Wei, P. Liao, H. Wu, X. Li, F. Pei, W. Li and Y. Wu, *Toxicol Appl Pharm*, 2008, **227**, 417-429.
46. Y. Wang, H. Tang, J. K. Nicholson, P. J. Hylands, J. Sampson and E. Holmes, *J Agr Food Chem*, 2005, **53**, 191-196.
47. M. Almar, J. G. Villa, M. J. Cuevas, J. A. Rodríguez-Marroyo, C. Avila and J. González-Gallego, *Free Radical Res*, 2002, **36**, 247-253.
48. S. J. Gatley and H. Sherratt, *Biochem. J*, 1977, **166**, 39-47.
49. D. Muldoon, E. Hassoun and S. Stohs, *Toxicon*, 1992, **30**, 977-984.
50. S. Smart, G. Fox, K. Allen, A. Swanson, M. Newman, G. Swayne, J. Clark, K. Sales and S. Williams, *Nmr Biomed*, 1994, **7**, 356-365.
51. R. W. Ansari, R. K. Shukla, R. S. Yadav, K. Seth, A. B. Pant, D. Singh, A. K. Agrawal, F. Islam and V. K. Khanna, *Neurotox Res*, 2012, **22**, 292-309.
52. J. Balkan, F. H. Parldar, S. Dogru-Abbasoglu, G. Aykaç-Toker and M. Uysal, *Eur J Gastroen Hepat*, 2005, **17**, 917-921.
53. H. P. Redmond, P. Stapleton, P. Neary and D. Bouchier-Hayes, *Nutrition*, 1998, **14**, 599-604.
54. Y.-R. Shi, D.-F. Bu, Y.-F. Qi, L. Gao, H.-F. Jiang, Y.-Z. Pang, C.-S. Tang and J.-B. Du, *Acta Pharmacol Sin*, 2002, **23**, 910-918.
55. S. M. Molchanova, S. S. Oja and P. Saransaari, *Neurochem Int*, 2005, **47**, 343-349.
56. F. Erman, J. Balkan, U. Cevikbaş, N. Kocak-Toker and M. Uysal, *Amino Acids*, 2004, **27**, 199-205.
57. R. Preston, D. Schnakenberg and W. Pfander, *J Nutr*, 1965, **86**, 281-288.
58. Y. Endo and K. Tsurugi, *J Biol Chem*, 1987, **262**, 8128-8130.
59. J. M. Lord, L. M. Roberts and J. D. Robertus, *Faseb J*, 1994, **8**, 201-208.
60. E. Holmes, J. K. Nicholson, A. W. Nicholls, J. C. Lindon, S. C. Connor, S. Polley and J. Connelly, *Chemometr Intell Lab*, 1998, **44**, 245-255.
61. Y. Wang, M. E. Bollard, J. K. Nicholson and E. Holmes, *J Pharmaceut Biomed*, 2006, **40**, 375-381.
62. M. Sieber, D. Hoffmann, M. Adler, V. S. Vaidya, M. Clement, J. V. Bonventre, N. Zidek, E. Rached, A. Amberg and J. J. Callanan, *Toxicol Sci*, 2009, **109**, 336-349.
63. J. D. Kopple, *J Nutr*, 2007, **137**, 1586S-1590S.
64. K. Mohib, Q. Guan, H. Diao, C. Du and A. M. Jevnikar, *Am J Physiol-Renal*, 2007, **293**, F801-F812.
65. A.-M. Myint, Y. K. Kim, R. Verkerk, S. Scharpé, H. Steinbusch and B. Leonard, *J Affect Disorders*, 2007, **98**, 143-151.
66. S. Okuda, N. Nishiyama, H. Saito and H. Katsuki, *J Neurochem*, 1998, **70**, 299-307.
67. J. Topczewska-Bruns, D. Pawlak, E. Chabielska, A. Tankiewicz and W. Buczko, *Brain Res Bull*, 2002, **58**, 423-428.

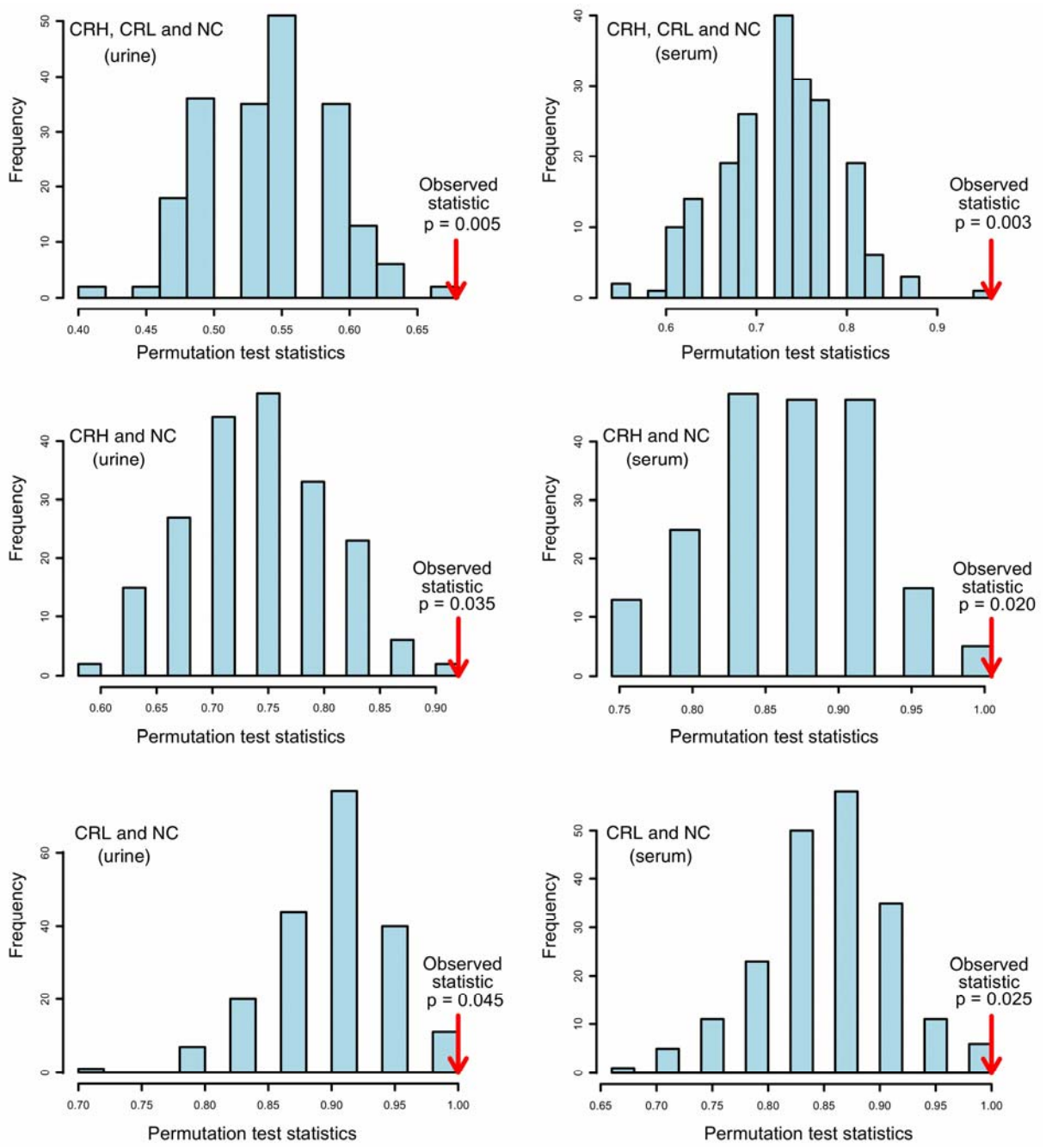

Fig.1 Histograms for permutation test scores of OSC-PLSDA models of NC, CRL and CRH group at week 7 on the basis of 200 permutations: the red arrow indicating the performance based on the original labels, significant for a p-value less than 0.05.

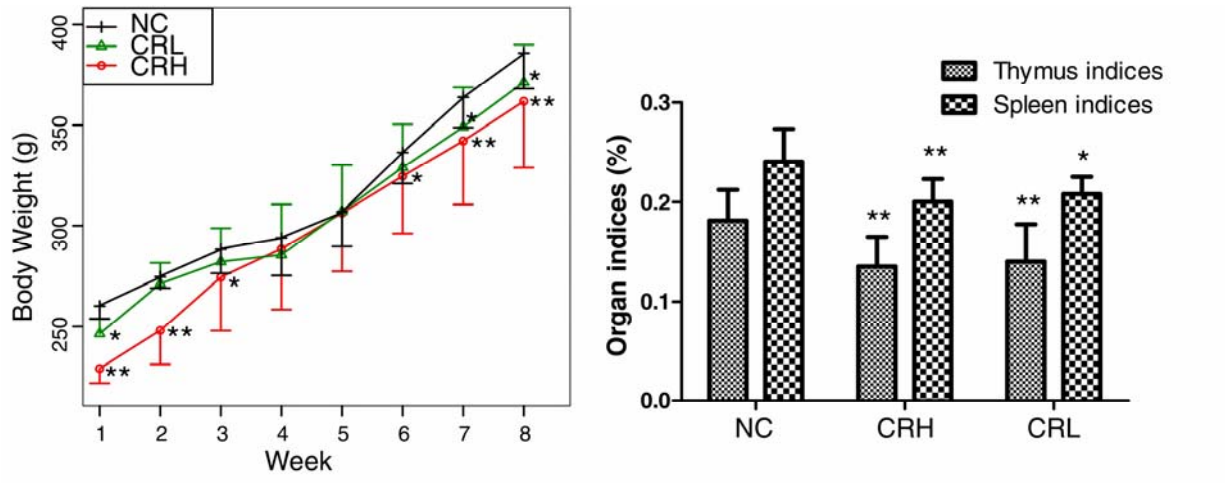

Fig.2 Body weight of all groups (A), and their spleen indices and thymus indices (B). *P < 0.05 and ** P < 0.01 vs NC

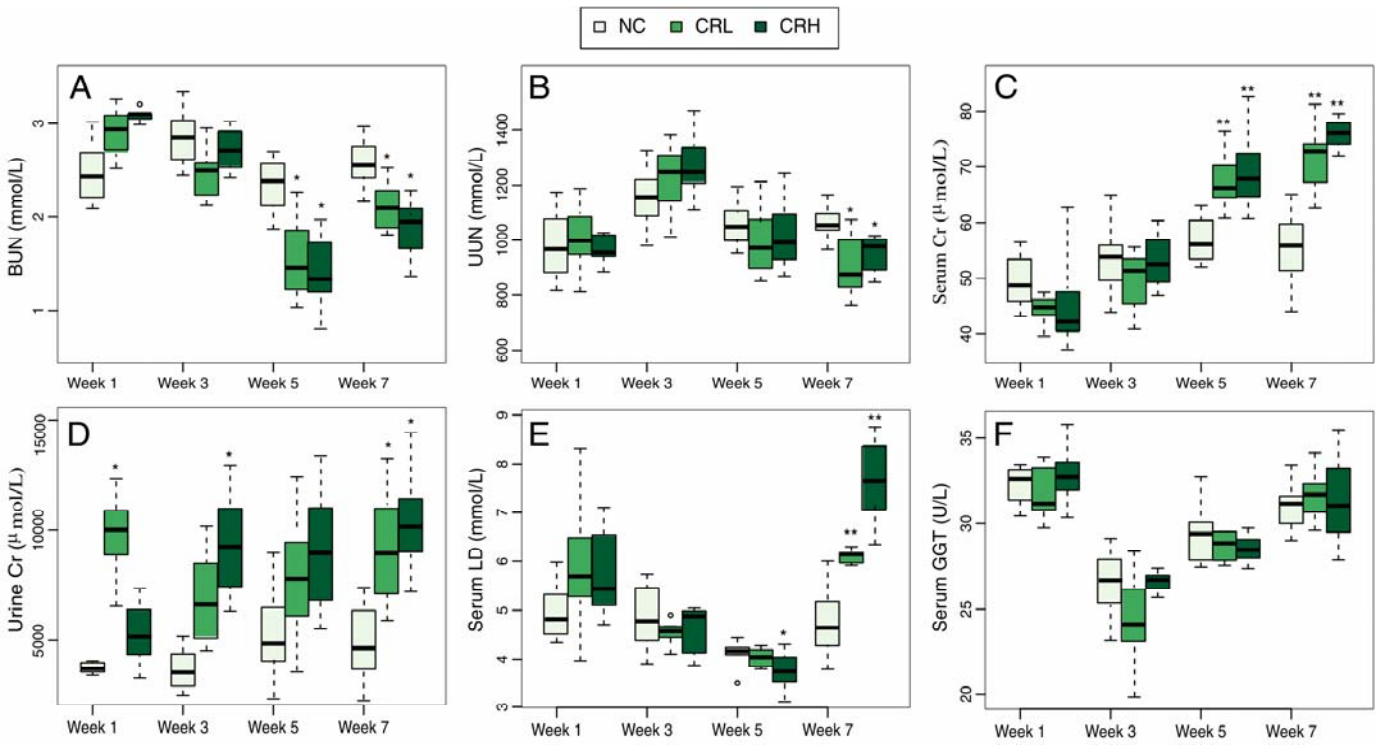

Fig.3 Boxplots for clinical chemistry results on BUN (A), UUN (B), serum Cr (C), urine Cr (D), serum LD (E), serum GGT (F) at week 1, 3, 5 and 7 after drug dosing. The bottom of each box, the line drawn in the box and the top of the box represent the 1st, 2nd, and 3rd quartiles, respectively. The whiskers extend to ± 1.5 times the interquartile range (from the 1st to 3rd quartile). Outliers are shown as open circle. All values are mean ± SD (n = 8). *P < 0.05 and ** P < 0.01 vs NC.

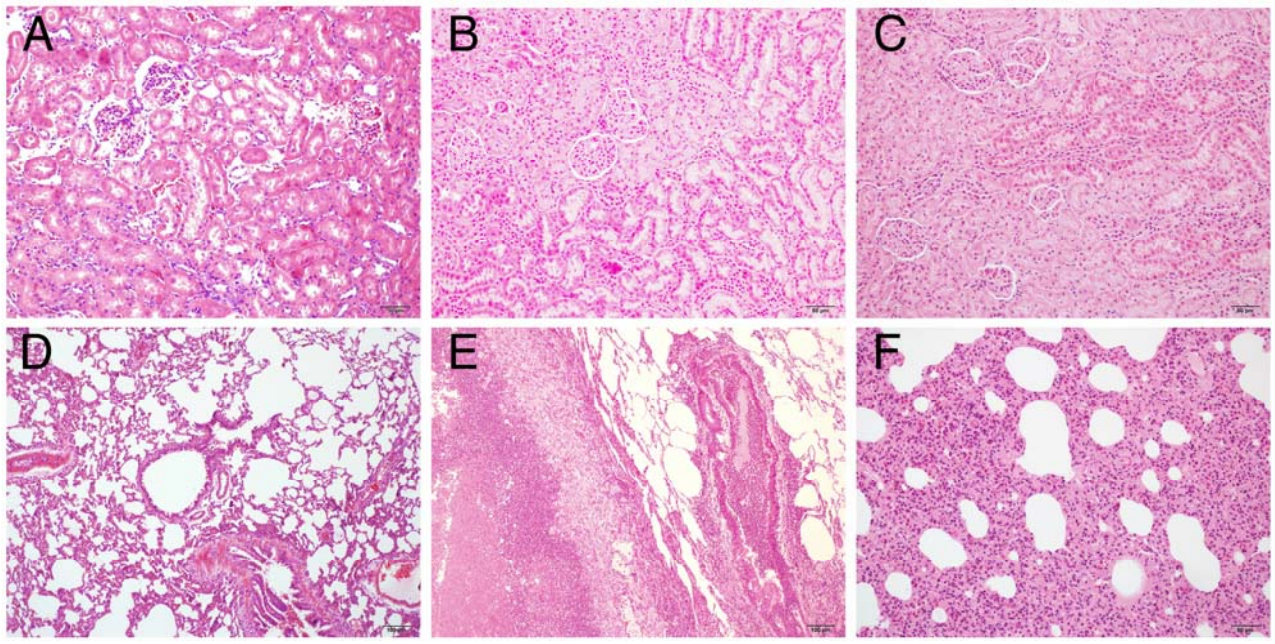

Fig.4 Histopathological photomicrographs of rat kidney (A, B and C) and lung sections (D, E and F), manifested from hematoxylin-eosin (HE) staining. Kidneys and lungs were taken out immediately from rats deeply anesthetized with chloral hydrate, fixed in 10% phosphate-buffered formalin for 12 h, embedded in paraffin, and sliced into 5 μm thickness. The sliced sections were stained with hematoxylin and eosin (H&E), and examined by light microscopy (A, B, C and F 200×, D and E 100×). CR treated kidney showed severe tubular necrosis and epithelial cell edema. Lung showed large amount of purulent exudates and severe alveolar wall thickening.

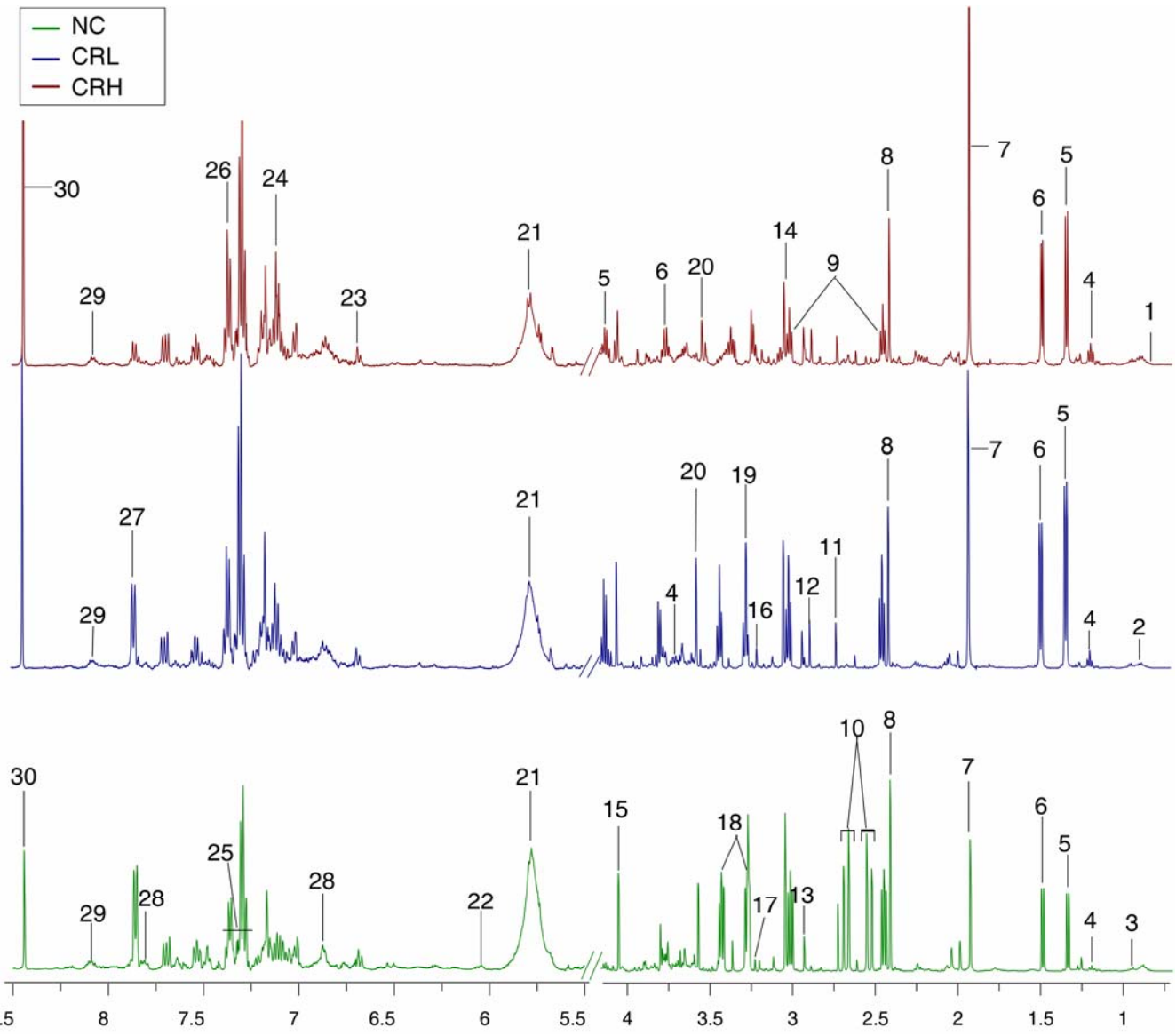

Fig.5 Typical 500 MHz NOESY ^{1}H NMR spectra of the urine samples from a CRH rat, a CRL rat and a NC rat on week 7. Metabolites: 1, isoleucine; 2, leucine; 3, valine; 4, ethanol; 5, lactate; 6, alanine; 7, acetate; 8, succinate 9, 2-oxoglutarate; 10, citrate; 11, dimethylamine; 12, trimethylamine; 13, N,N-dimethylglycine; 14, creatine; 15, creatinine; 16, choline; 17, phosphocholine; 18, taurine; 19, betaine; 20, glycine; 21, urea; 22, allantoin; 23, kynurenic acid; 24, tyrosine; 25, phenylalanine; 26, tryptophan; 27, hippurate; 28, kynureninie; 29, trigonelline; 30, formate

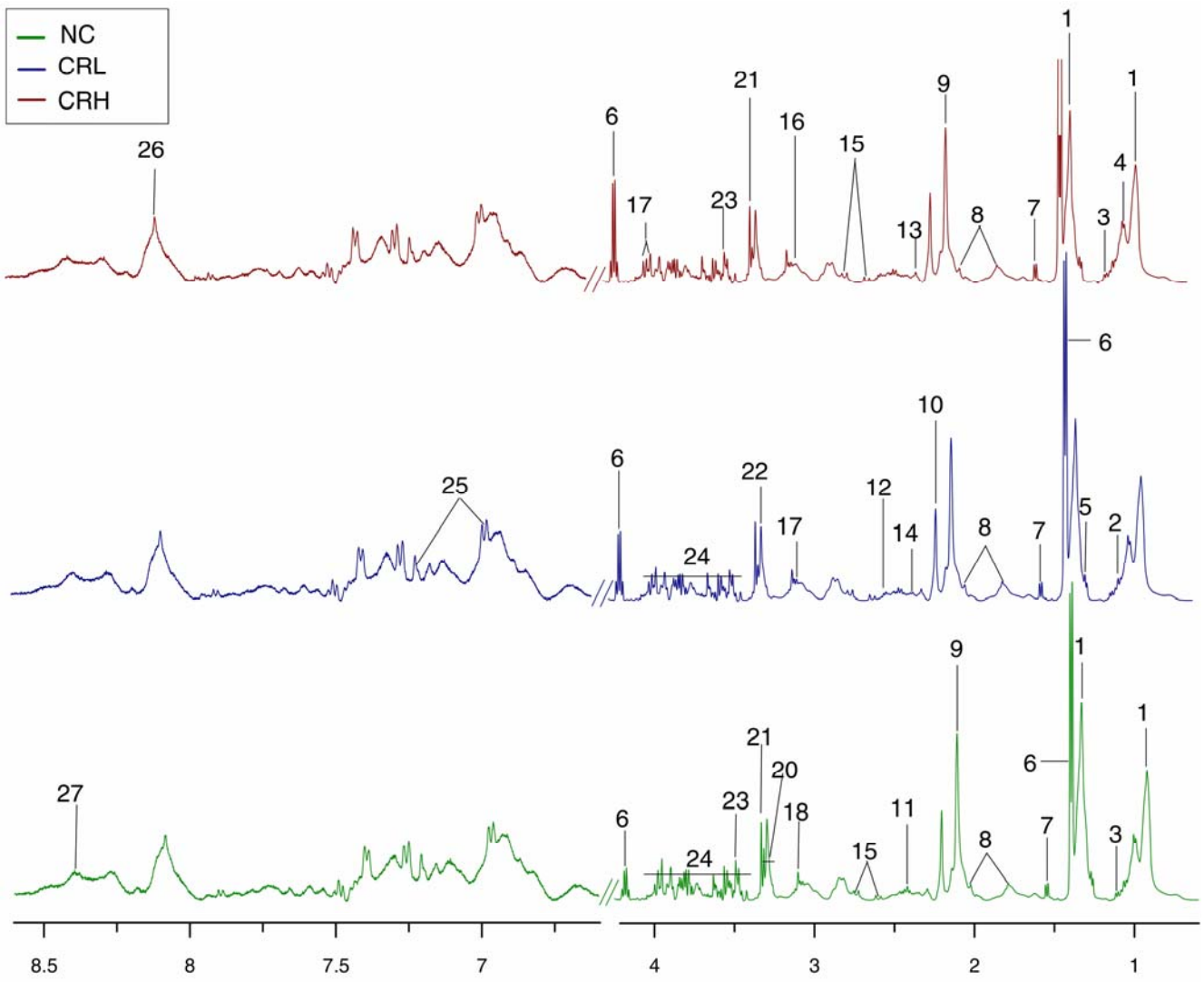

Fig.6 Typical 500 MHz CPMG ^{1}H NMR spectra of the serum samples from a CRH rat, a CRL rat and a NC rat on week 7. Metabolites: 1, lipoproteins (LDL/VLDL); 2, leucine; 3, isoleucine; 4, valine; 5, 3-hydroxybutyrate (3HB); 6, lactate; 7, alanine; 8, arginine; 9, N-Acetyl glycoproteins; 10, O-Acetyl glycoproteins; 11, glutamate; 12, glutamine; 13, acetoacetate; 14, pyruvate; 15, citrate; 16, cysteine; 17, creatine; 18, creatinine; 19, choline; 20, taurine; 21, betaine; 22, glycerophosphorylcholine (GPC); 23, glycine; 24, glucose; 25, tyrosine; 26, trigonelline; 27, formate

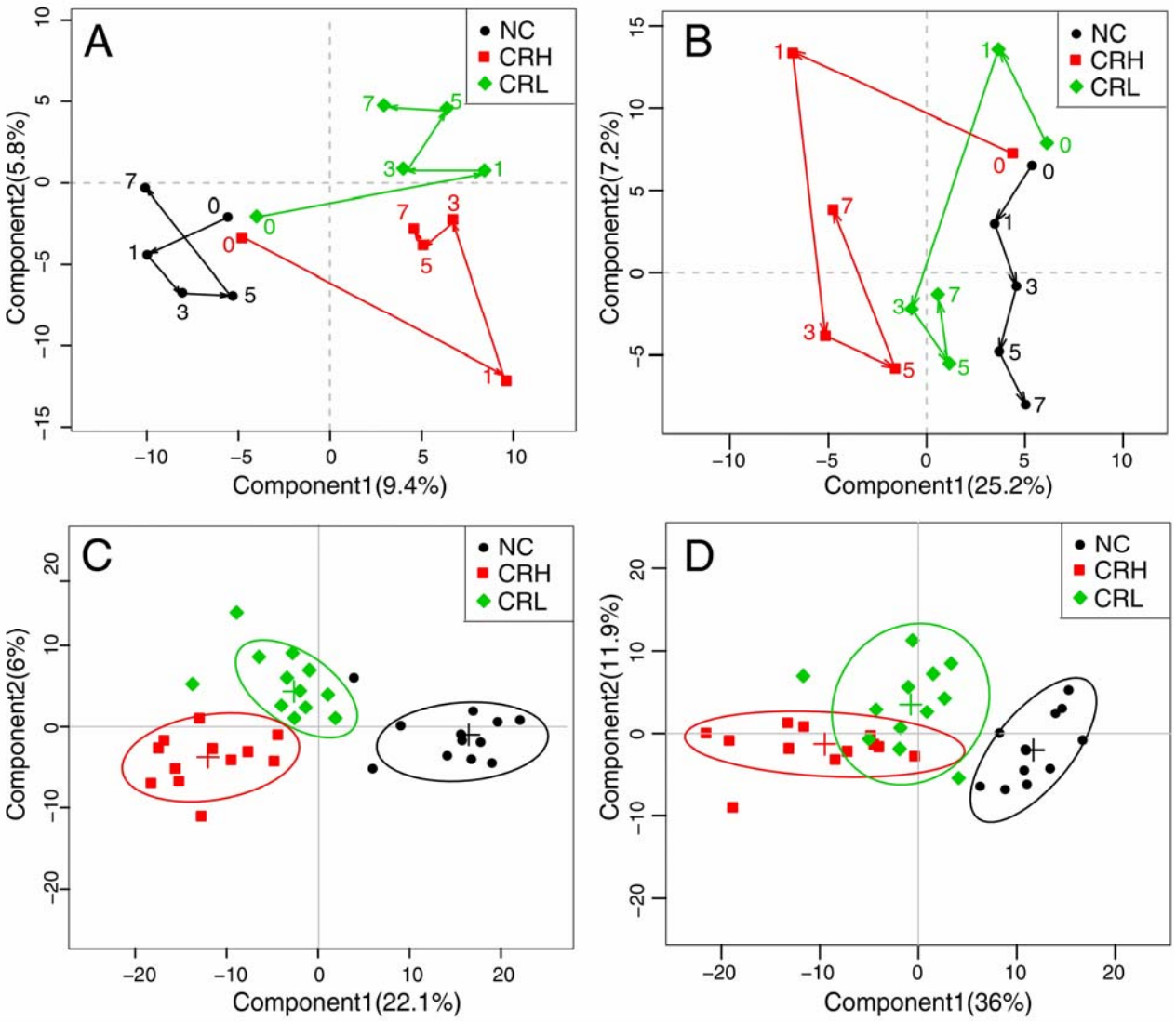

Fig.7 OSC-PLSDA trajectory score plots based on the data of urine NOESY ^{1}H NMR spectra (A) and serum CPMG ^{1}H NMR spectra (B) of rats in different groups in 4 time points (n=12 for each group). The number 0, 1, 3, 5 and 7 denoted the week of administration. OSC-PLSDA score plots obtained from ^{1}H NMR NOESY urine spectral data (C) and ^{1}H NMR CPMG serum spectral data (D) for rats in NC (filled circle), CRH (filled square) and CRL (filled diamond) on week 7 (n=12).

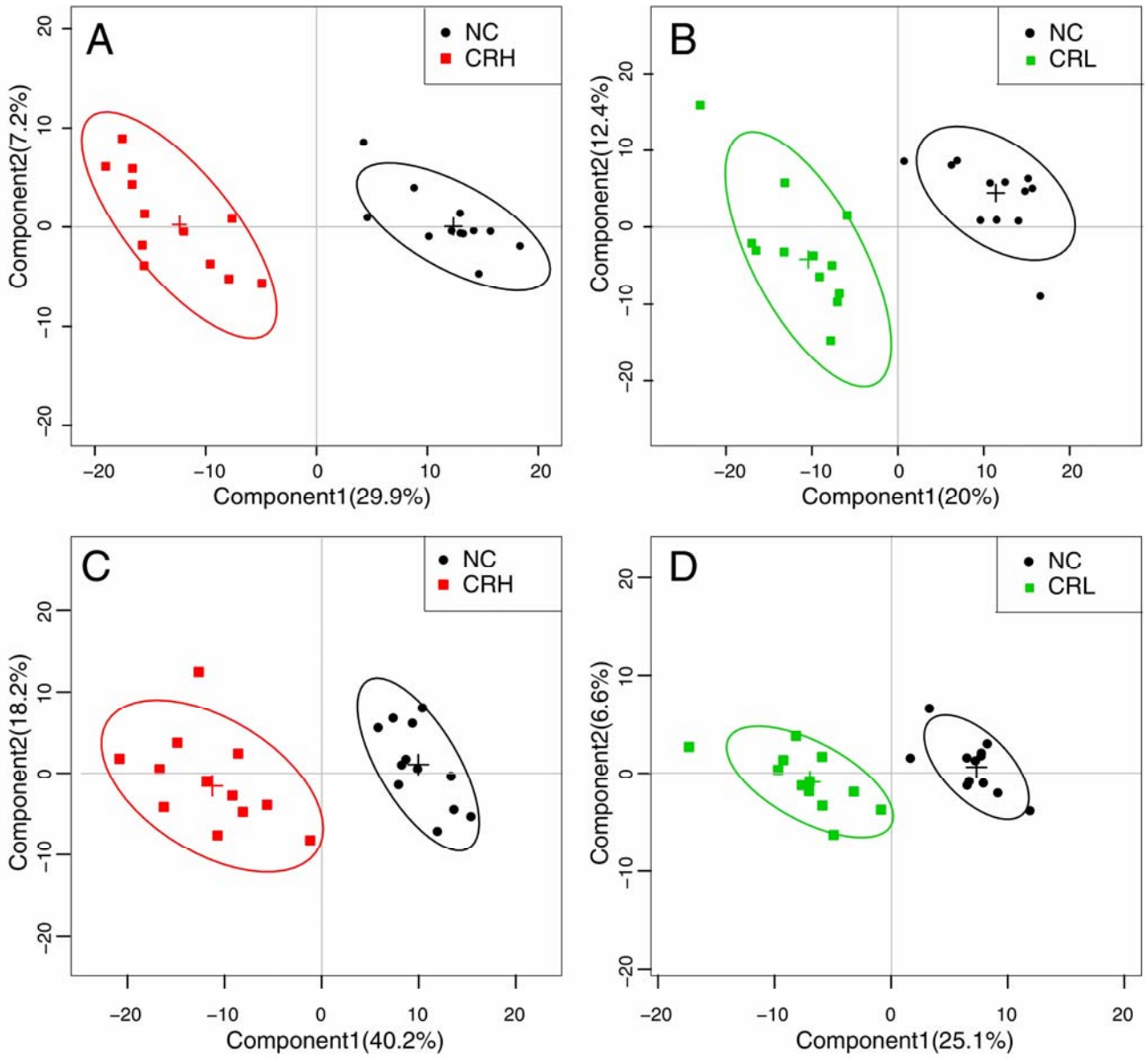

Fig.8 Score plots from OSC-PLSDA analysis of NMR data from urine and serum of rats: urine of CRH and NC (n=12) (A), and of CRL and NC (n=12) (B); serum from CRH and NC (n=12) (C), and from CRL and NC (D) (n=12).

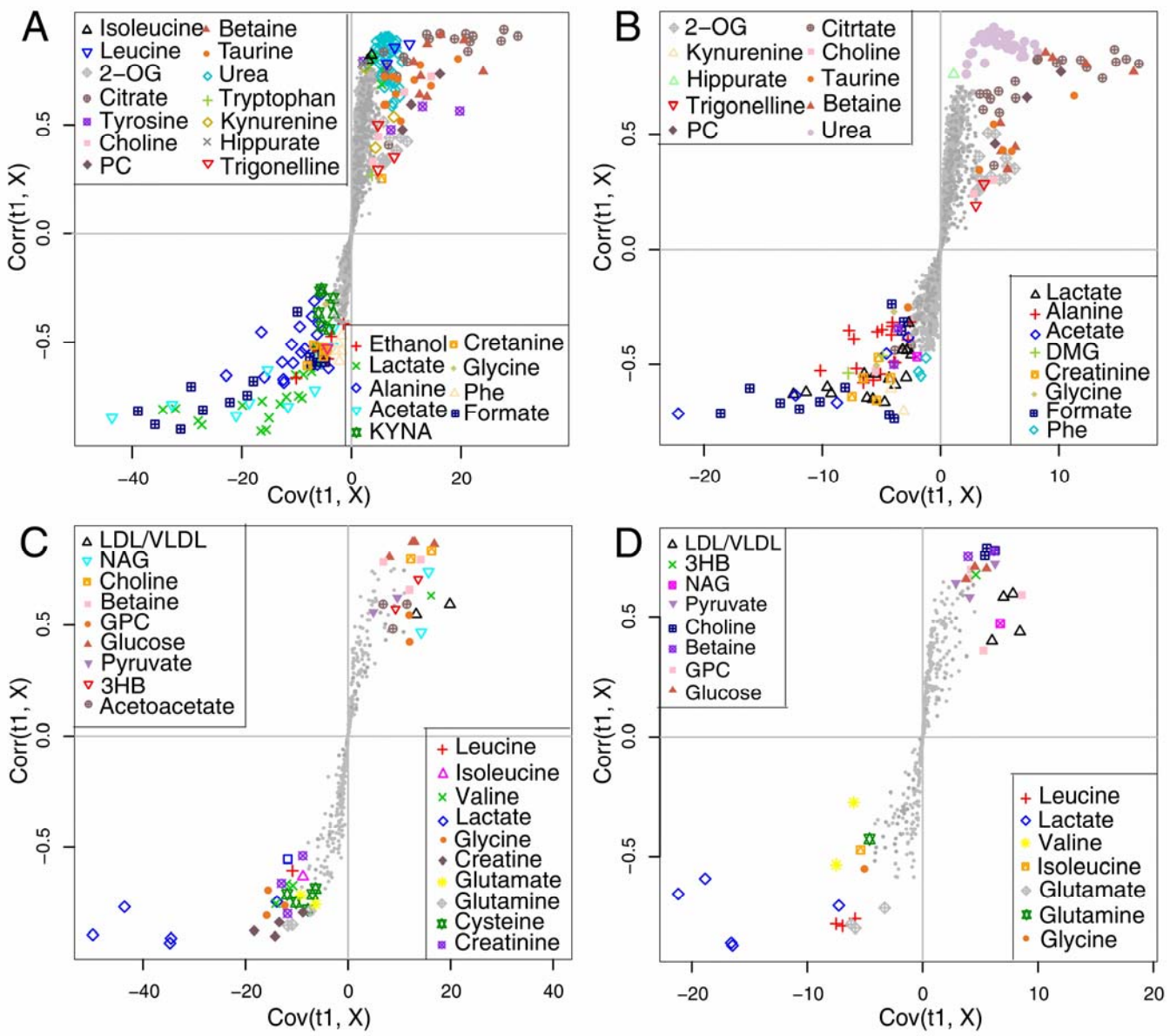

Fig.9 S-plots for OSC-PLSDA analysis of NMR metabolomic profiles of rat urine and serum on week 7: urine of CRH vs NC (A), and of CRL vs NC (B); serum from CRH vs NC (C), and from CRL vs NC (D) (n=12). 2-OG, 2-oxoglutarate; PC, phosphocholine; GPC, glycerophosphorylcholine; DMG, dimethylglycine; phe, phenylalanine; LDL/VLDL, Low density lipoprotein/Very low density lipoproteins; NAG, N-Acetyl glycoproteins; 3HB, 3-hydroxybutyrate; KYNA, kynurenic acid.

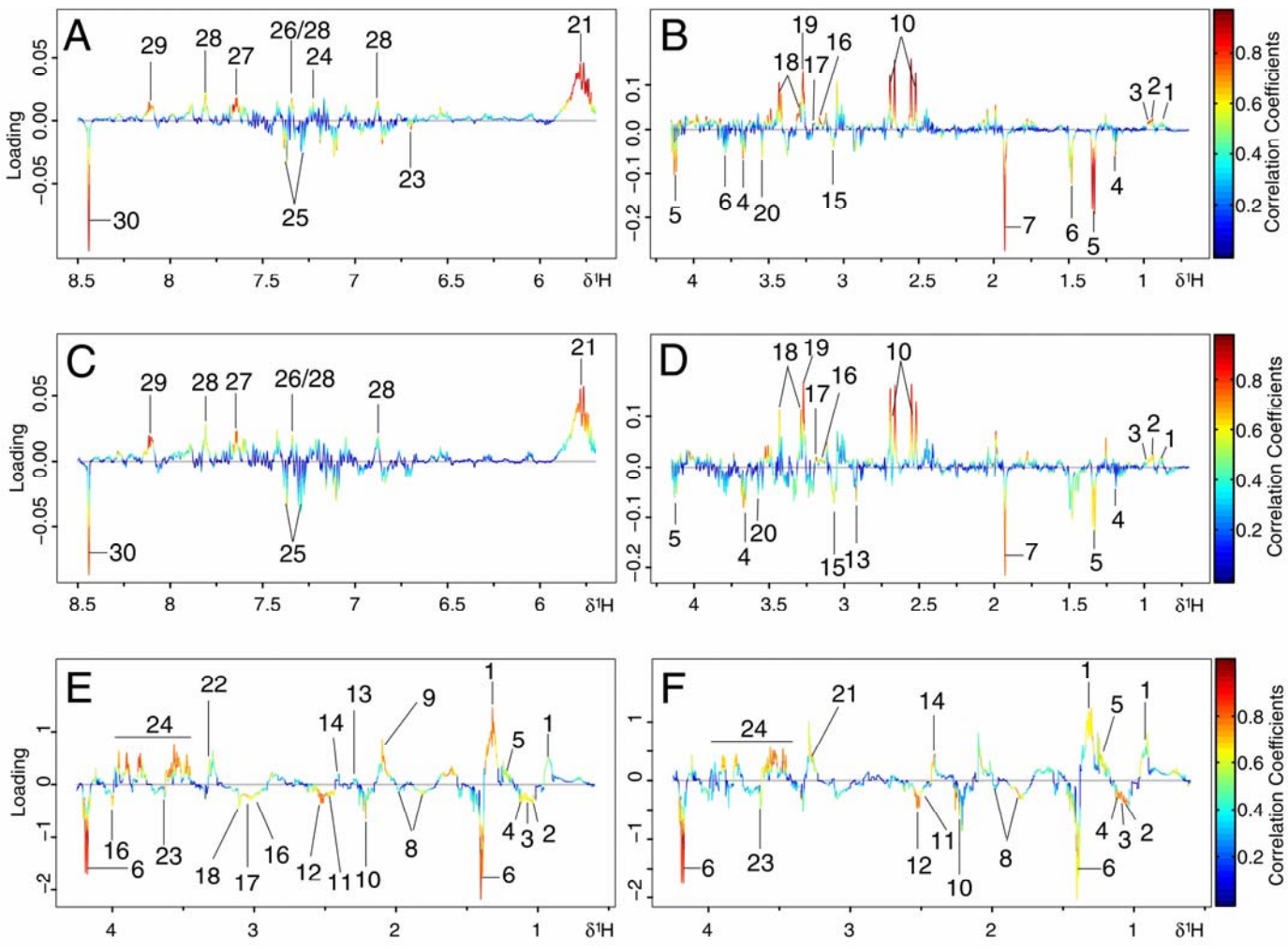

Fig.10 Color-coded loading plots according to the OSC-PLSDA analysis with the metabolites labeled: urine of CRH and NC (A and B), and of CRL and NC (C and D); serum from CRH and NC (E), and from CRL and NC (F) (n=12). Blue: lowest, no statistically significant difference between the groups; Red: highest, statistically significant.

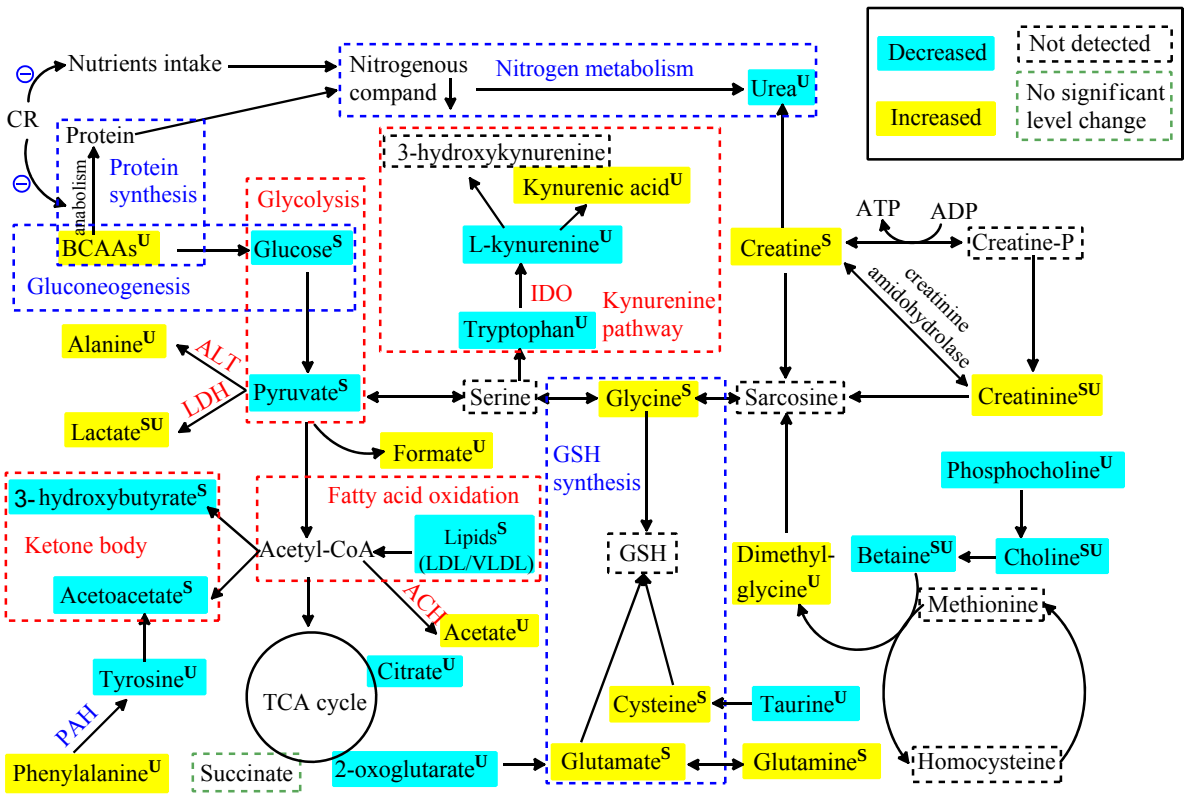

Fig. 11 Schematic diagram of the perturbed metabolic pathways detected by NMR analysis, showing the interrelationship of the identified metabolic pathways. "–" means inhibition effect. The words in blue mean inhibited pathways and enzymes, words in red mean promoted pathway and enzymes. Metabolites with superscript "^{U}" means observed significant level change from urine; "^{S}" means observed significant level change from serum; "^{SU}" means observed significant level change from both serum and urine.

Table 1 The OSC-PLSDA model parameters of comparison among different groups on week 7

	R^2Y	Q^2Y	P (Permutated)
CRH, CRL and NC (urine)	0.902	0.741	0.005
CRH, CRL and NC (serum)	0.815	0.596	0.003
CRH and NC (urine)	0.993	0.881	0.035
CRH and NC (serum)	0.964	0.728	0.020
CRL and NC (urine)	0.992	0.843	0.045
CRL and NC (serum)	0.954	0.682	0.025

Table 2 Identified metabolites of the urine from different groups.

No.	Mebabolite	Assignments	Chemical shift[a] (ppm)	CRH vs NC fold change[b]; *P*		CRL vs NC fold change[b]; *P*	
1	Isoleucine	δCH_3,βCH_3, γCH2	0.93(t), 1.02(d), 1.46(m)	0.602	0.029	0.763	0.036
2	Leucine	δCH_3,βCH_3, βCH,αCH	0.97(t), 1.00(t), 1.71(m),3.74(m)	0.593	0.017	0.687	0.046
3	Valine	γCH_3,γCH_3, βCH,αCH	0.97(d), 1.07(d), 2.26(m),3.60(d)	0.683	0.019	0.887	0.048
4	Ethanol	CH_3, CH_2	1.19(t),3.67(q)	1.399	0.008	1.091	0.015
5	Lactate	CH_3,CH	1.35(d), 4.15(q)	2.307	<0.001	1.534	<0.001
6	Alanine	βCH_3,αCH	1.51(d), 3.78(q)	1.645	0.007	1.560	0.012
7	Acetate	CH_3	1.93(s)	2.499	<0.001	1.649	<0.001
8	Succinate	CH_2	2.43(s)	0.984	~	0.914	~
9	2-oxoglutarate	γCH_2,βCH_2	2.45(t),3.02(t)	0.745	0.043	0.796	0.049
10	Citrate	$1/2CH_2$,$1/2CH_2$	2.60(AB), 2.72(AB)	0.435	<0.001	0.588	<0.001
11	Dimethylamine	CH_3	2.73(s)	0.950	~	0.914	~
12	Trimethylamine	CH_3	2.88(s)	0.932	~	0.867	~
13	N,N-Dimethylglycine	CH3	2.93(s)	1.287	~	1.611	0.036
14	Creatine	CH_3,CH_2	3.01(s),3.95(s)	0.863	0.026	0.934	~
15	Creatinine	CH_3,CH_2	3.05(s),4.05(s)	1.584	0.014	1.051	0.029
16	Choline	$N(CH_3)_3$,$N–CH_2$	3.19(s), 3.51(m)	0.695	<0.001	0.639	0.004
17	Phosphocholine	CH_3	3.21(s)	0.705	0.006	0.882	<0.001
18	Taurine	$SO_3–CH_2$,$CH_2–NH_2$	3.27(t), 3.42(t)	0.680	<0.001	0.783	<0.001
19	Betaine	CH_3	3.26(s)	0.577	<0.001	0.706	<0.001
20	Glycine	CH_2	3.57(s)	1.144	0.004	1.189	0.008
21	Urea	NH_2	5.80(br)	0.508	<0.001	0.516	<0.001
22	Allantoin	NH_2	6.04(br)	0.981	~	0.975	~
23	Kynurenic acid	CH	6.7(s),7.34(m),7.54(d), 7.63(m),7.91(m)	1.396	0.014	1.054	0.046
24	Tyrosine	CH	6.89(d),7.20(t)	0.628	0.028	0.912	0.046
25	Phenylalanine	CH	7.32(m),7.40(m)	2.368	0.027	1.595	0.039
26	Tryptophan	CH	7.36(s)	0.844	0.025	0.905	0.043
27	Hippurate	CH	7.55(t),7.63(t),7.83(d)	0.818	<0.001	0.875	<0.001
28	Kynurenine	CH	6.84(m),7.36(m),7.79(m)	0.888	0.019	0.974	0.030
29	Trigonelline	CH	8.08(t)	0.789	<0.001	0.863	<0.001
30	Formate	CH	8.44(s)	2.742	<0.001	1.796	<0.001

[a] s, singlet; d, doublet; t, triplet; q, quartet; m, multiplet; br, broad singlet.

[b] "~" means no significant change.

Table 3 Identified metabolites of the serum in different groups.

No.	Mebabolite	Assignments	Chemical shift[a] (ppm)	CRH vs NC		CRL vs NC	
				fold change[b]; *P*		fold change[b]; *P*	
1	Lipoproteins (LDL/VLDL)	$CH_3(CH_2)_n$ CH3CH2CH2C=	0.89(m), 1.20-1.30(m)	0.729	0.007	0.861	0.024
2	Leucine	δCH_3, δCH_3 γCH, αCH2	0.97(t), 1.00(t) 1.71(m), 3.74(m)	1.290	0.035	1.070	0.028
3	Isoleucine	δCH_3, βCH_3, γCH_2	0.93(t), 1.02(d), 1.46(m)	1.256	0.024	1.136	0.022
4	Valine	γCH_3, γCH_3, βCH, αCH	1.03(d), 1.07(d), 2.26(m), 3.60(d)	1.168	0.028	1.086	0.015
5	3-hydroxybutyrate	γCH_3, βCH, αCH2	1.19(d), 4.23(m), 2.31(dd), 2.38(dd)	0.274	0.032	0.431	0.021
6	Lactate	CH_3, CH	1.35(d), 4.15(q)	1.719	<0.001	1.423	0.011
7	Alanine	βCH_3, αCH	1.51(d), 3.78(q)	1.275	~	1.006	~
8	Arginine	γCH_2, βCH_2	1.75(m), 1.91(m)	1.216	0.045	1.014	0.032
9	N-acetyl-glycoproteins	CH_3	2.09(s)	0.757	0.017	0.854	0.048
10	O-acetyl-glycoproteins	OHCHCH3	2.19(s)	1.193	0.012	1.004	~
11	Glutamate	βCH_2, γCH_2	2.08(m), 2.46(m)	1.229	0.002	1.113	0.009
12	Glutamine	βCH_2, γCH_2	2.13(m), 2.50(m)	1.308	<0.001	1.446	<0.001
13	Acetoacetate	CH_3	2.27(s)	0.726	0.042	0.846	0.046
14	Pyruvate	βCH_3	2.44(s)	0.787	0.048	0.957	0.021
15	Citrate	$1/2CH_2$, $1/2CH_2$	2.60(AB), 2.72(AB)	0.800	~	0.950	~
16	Cysteine	CH_2,CH	3.06(m),3.97(dd)	1.221	0.037	1.101	0.045
17	Creatine	CH_3, CH_2	3.07(s), 3.92(s)	1.302	0.027	1.204	0.033
18	Creatinine	CH_3, CH_2	3.10(s), 4.05(s)	1.226	0.034	1.372	0.041
19	Choline	$N(CH_3)_3$, N-CH_2	3.20(s), 3.51(m)	0.611	0.041	0.933	0.047
20	Taurine	SO_3-CH_2, CH_2-NH_2	3.28(t), 3.42(t)	0.651	~	0.667	~
21	Betaine	$N(CH_3)_3$	3.30(s)	0.751	0.034	0.841	0.023
22	GPC	$N(CH_3)_3$	3.27(s)	0.967	0.026	0.875	0.048
23	Glycine	CH2	3.54(s)	1.146	0.039	1.217	0.023
24	Glucose	CH	3.45-4.0(m)	0.726	<0.001	0.791	<0.001
25	Tyrosine	H_3/H_5, C_5H/C_6H	6.89(d), 7.20(t)	/	/	/	/
26	Trigonelline	CH	8.08(t)	/	/	/	/
27	Formate	CH	8.44(s)	/	/	/	/

[a] s, singlet; d, doublet; t, triplet; q, quartet; m, multiplet; br, broad singlet.

[b] "~" means no significant change; "/" means data not shown.